International Journal of Engineering Research & Technology (IJERT)
ISSN: 2278-0181
Vol. 2 Issue 12, December - 2013

CFD Simulation of Pickup Van

Mahesh H. Dasar[a], Deepak J. Patil[b], Raviraj M[c]

[a] Assistant Professor, Annasaheb Dange College of Engineering & Technology, Ashta, Sangli, Maharastra, India,

[b] Project Lead, Zeus Numerix Pvt. Ltd. Pune, India,

[c] Assistant Professor, Fabtech College of Engineering & Research, Sangola, Pandarpur road, Maharastra,

ABSTRACT

Broadly, the objective of this study is to carry out 3-Dimensional, incompressible, steady-state CFD simulation of a simplified pickup van with smooth underbody and without side mirrors, by employing pressure based commercial software CFDExpert-Lite™ to carry out Reynolds Averaged Navier-Stokes (RANS) based computations to investigate the aerodynamics of pickup van. k-ε turbulence model with standard wall functions and structured CFD domain is used in the simulation to study the flow parameters in and around the wake region and a detailed study of the quantitative data set for validation of numerical simulations has been conducted. Simulations were carried out at moderate Reynolds numbers (~3×10^5) and the measured quantities include: the pressure distributions on the symmetry plane and the velocity profiles near the wake.

The good comparisons obtained for experimental and numerical data throughout this study mean that CFD analysis could be profitably used instead of wind tunnel test.

Keywords: CFD, CFDExpert-Lite™, 3 Dimensional, Turbulence model, wind tunnel.

1. INTRODUCTION

Pickup vans are one of the more popular vehicles in use today yet it has received very little attention in car aerodynamics literature. The aerodynamics of pickup vans is more complex than any other open bed trucks, because the short length of the bed can result in interaction of the bed walls and tailgate with the separated shear layer formed at the edge of the cab. The present study is to gain a better understanding of the flow structure near the wake region, since the theories on the aerodynamics are yet to mature and wind tunnel experiments cost long periods and great expenses, the numerical simulation based on computational fluid dynamics (CFD) is a good approach to adopt.

The complexity of the flow makes drag prediction tools, including CFD based methods, unreliable. The main goal of the present research is to gain a better understanding of pickup truck aerodynamics using detailed flow field measurements

Computational Fluid Dynamics (CFD) has gained popularity as a tool for many airflow situations including road vehicle aerodynamics. This trend, to bring CFD to bear on vehicle aerodynamic design issues, is appropriate and timely in view of the increasing competitive and regulative pressures being faced by the automotive industry. Three-dimensional transient

aerodynamic flow model development occurs in an environment influenced by numerical and turbulence modeling uncertainties, among others. In order to assess the accuracy of the aerodynamic CFD flow computations, a comprehensive comparison between the CFD results and measurements of the aerodynamic flow structures over generic pickup truck geometry is undertaken. Detailed flow field comparison includes surface pressures and velocity fields in the near-wake region.

2. METHODOLOGY

Vehicle Geometry

The model represents a 1:12 scale of the full-scale pickup truck. Schematics of the pickup truck model with the pertinent dimensions are depicted in Figure 2.1. The length of the model is 0.432 m, the width is 0.152 m, and the height is 0.1488 m [1] [5]. The model was designed with a smooth underbody, enclosed wheel-wells and without openings for cooling airflow. An identical surface model was generated for the CFD simulations. Once the surfaces for the model are created, they are used to generate a three-dimensional grid for the CFD calculations.

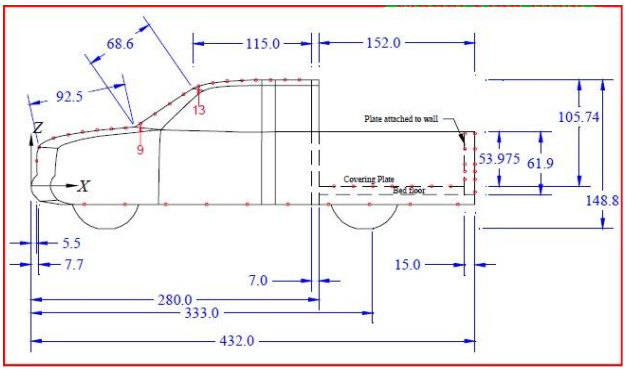

Fifure 2.1 Pickup Van Dimensions

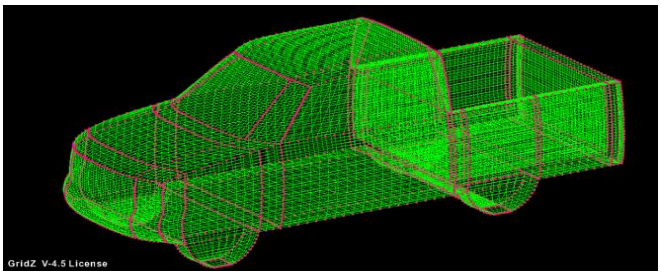

Figure 2.2 Pickup van geometry

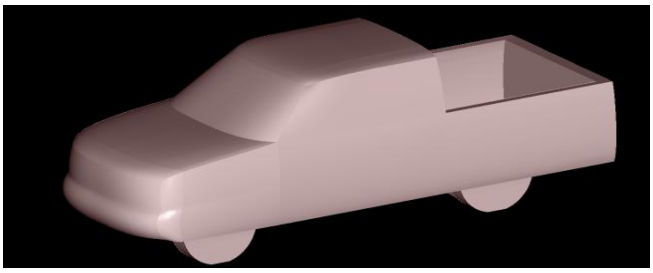

Figure 2.3 Pickup van geometry.

Meshing:

In the computational domain, the vehicle is kept such that the point lying on the ground in the plane of symmetry is the origin. The length of the domain upstream of the vehicle, up to the inlet boundary, is 5 times the length of the vehicle (0.432 m). Length of the domain in the downstream direction, up to the outlet boundary, 10 times the length of the vehicle. Height of the domain measured from the topmost point of the vehicle is 5 times the length of the vehicle. In the lateral direction, boundary of the domain is located 5 times the length of the vehicle.

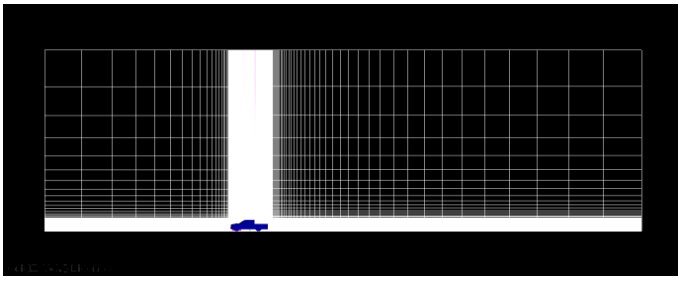

Figure 2.4 Flow Domain Side View

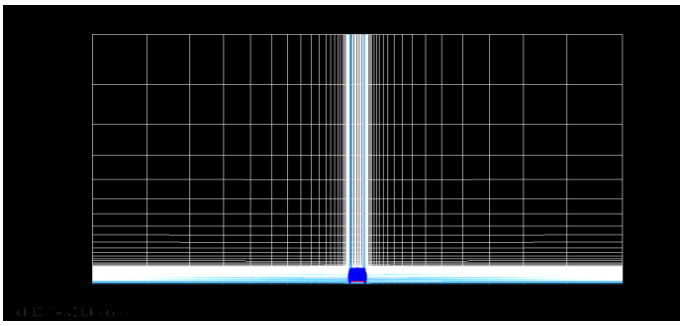

Figure 2.5 Flow Domain Front View

Generation of multi-block structured grids for the simulation requires the topology of the domain (i.e. position and neighborhood of blocks around the vehicle as shown in figure 2.6). Finer grids are required at the areas of importance, which include regions close to the surface of the vehicle and the region behind the cab and the tailgate. A topology of 270 surface blocks covered the entire vehicle. A total of 2158530 cells were put on the surface of the vehicle. A topology with 270 three-dimensional blocks commensurate with 98 surface blocks was arrived at for the current problem. The grids were then smoothened using the Laplace smoothener. Exponential clustering function was used to put 2nd grid points close to the wall within 0.011 mm (Table: 2.1). The clustered grids in one of such block are shown in Figure: 09. The total number of mesh points used in this study was about 2.1 Million.

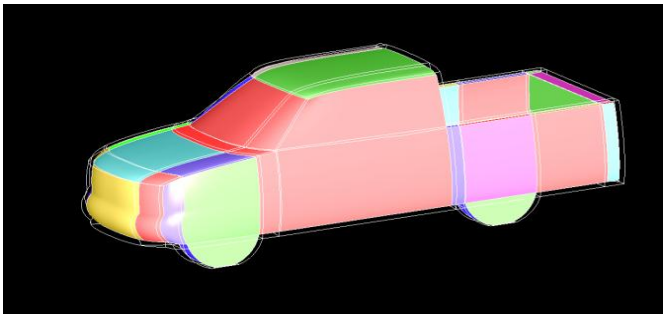

Figure 2.6 Neighborhood of blocks around the vehicle

Table 2.1 Computational meshes Considered for the Pickup van simulation.

Test Case	Number of Cells	Total Grid Points	Avg. First Cell Distance
Pickup Van_18	2158530	2221690	0.011
Pickup Van_25	2158530	2221690	0.011
Pickup Van_30	2158530	2221690	0.011

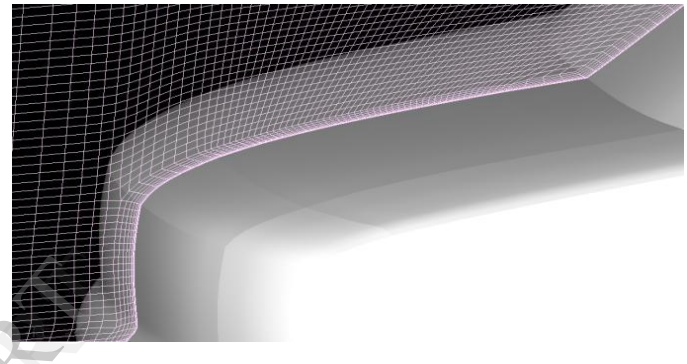

Figure 2.7 Clustered mesh on bonnet of the pickup van

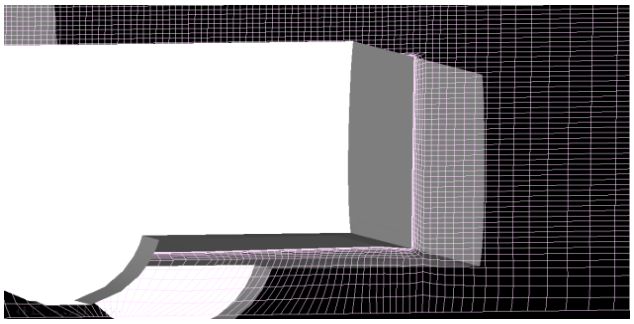

Figure 2.8 Clustered mesh on tailgate of the pickup van

Solver:

In the present study all the computations for the computational domain have been carried out using a three dimensional RANS model with an industry standard finite volume based CFD code, CFDExpert-Lite. The set of equations solved by CFDExpert-Lite are the unsteady

Navier Stokes equation in their conservation form for turbulent flows, the instantaneous equations are averaged leading to additional terms. Assuming the flow to be steady, incompressible and turbulent the governing equations are solved based on finite volume approach

Governing equations

General governing equations for incompressible flows are as follows:

Continuity

$$\nabla . V = \frac{\partial u}{\partial x} + \frac{\partial v}{\partial y} + \frac{\partial w}{\partial z} = 0$$

Momentum

$$\rho\left(\frac{\partial}{\partial t} + \nabla . V\right)u = -\frac{\partial p}{\partial x} + \mu\nabla^2 u + \rho f_x$$

$$\rho\left(\frac{\partial}{\partial t} + \nabla . V\right)v = -\frac{\partial p}{\partial y} + \mu\nabla^2 v + \rho f_y$$

$$\rho\left(\frac{\partial}{\partial t} + \nabla . V\right)w = -\frac{\partial p}{\partial z} + \mu\nabla^2 w + \rho f_z$$

(7.4)

Turbulence Modeling

The standard $k-\varepsilon$ model is used for the simulations. Since the boundary condition for $k-\varepsilon$ is not well defined near the wall, one uses the law of the wall as the relation between velocity and surface shear stress. Evaluation of shear stress depends on whether the near wall cell lies in the viscous sub layer or in the fully turbulent region as decided by non-dimensional distance y^+.

Boundary and Initial Conditions

The inlet boundary was based on constant total pressure and enthalpy. Static pressure at the inlet is 101300 Pa and the inlet Mach No is 0.1, these quantities are used to calculate the total pressure. Similarly density of air was set to 1.225 kg/m^3 for calculation of inlet enthalpy. The outlet static pressure is held constant at 101300 Pa.

All the grid points in the domain are given a uniform value of 18, 25, & 30.0 m/s (Three test cases) as initial velocity values in the x direction, whereas y-velocity and z-velocity components are kept zero initially. Solution moves towards steady-state from the specified initial conditions by marching in pseudo time.

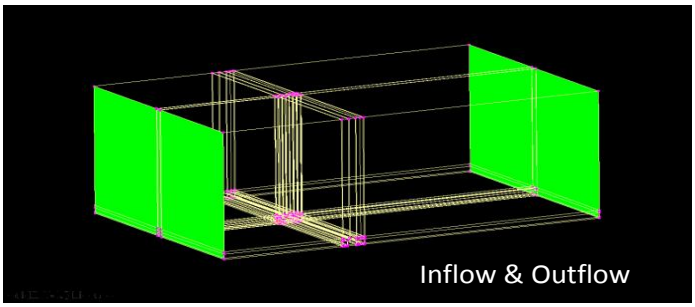

Figure 2.9 Boundary conditions: Inlet & Outlet

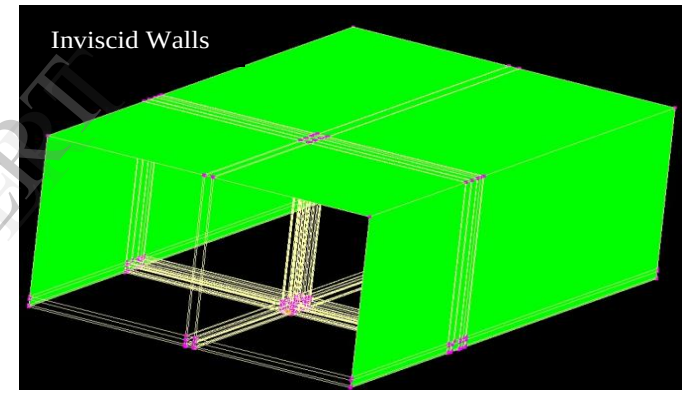

Figure 2.10 Boundary conditions: Inviscid walls

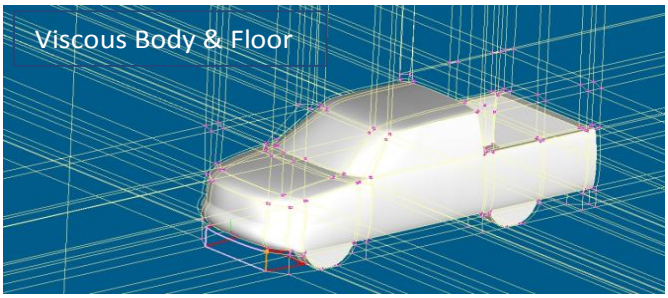

Figure 2.11 Boundary conditions: Viscous Floor & Viscous Body

Table 2.2 Boundary Conditions

FACES	BOUNDARY CONDITIONS
Front Face	Inflow

Rear Face	Inflow
Right Face	Inviscid Wall
Left Face	Inviscid Wall
Top Face	Inviscid Wall
Floor	Viscous Wall
Vehicle Body	Viscous Wall

Solver Setup

Fluid Properties:

1. Density = 1.225 kg/m³
2. Dynamic Viscosity = $1.7894*10^{-5}$
3. Pressure Velocity Coupling – SIMPLE {Semi-Implicit Method for Pressure-Linked Equations}

Reconstructing:

4. Upwind Scheme = UDS
5. Scheme Order = SECOND
6. Turbulence Model: k-ε High Reynolds number with Std. wall function

Initial conditions:

7. Initial Pressure = 0.0
8. Initial Velocity X = 30, 25, 18 Y=0 Z=0
9. Initial Turbulence Intensity = 2.0
10. Initial Eddy Viscosity Ratio =10.0

3. RESULTS AND DISCUSSION

Mean pressure measurements

The mean pressure coefficient measured along the symmetry plane of the model is shown in Figures at Reynolds numbers 1.74 × 105, 2.36 × 105 and 2.88 × 105, respectively, which correspond to wind tunnel speeds of 18, 25 and 30 *m/s*, respectively, and the results are validated with the experimental results.

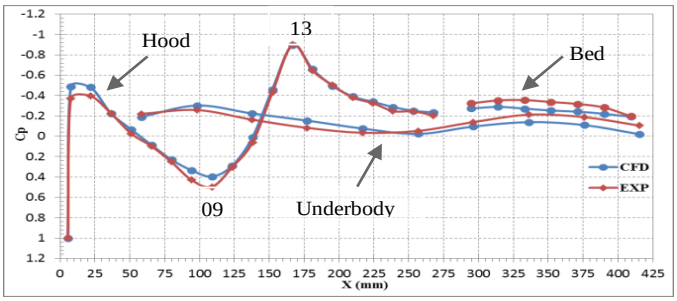

Figure 3.1 (a) Mean pressure coefficient distribution measured on the symmetry plane of the pickup At 18 m/s

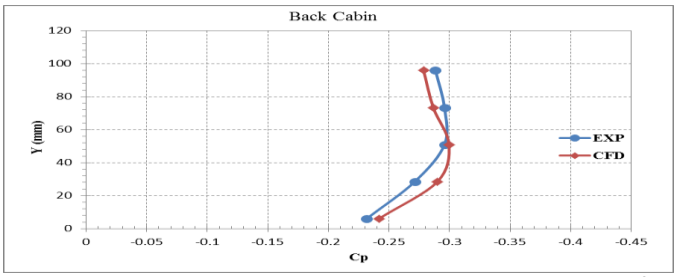

Figure 3.1 (b): Pressure distributions measured on the symmetry plane of the back surface of the cabin at 18 m/s

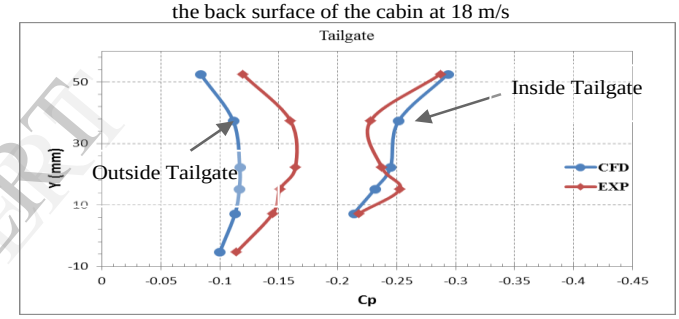

Figure 3.1 (c): Pressure coefficient distribution measured on the symmetry plane of the inside and outside surfaces of the tailgate of the pickup truck at 18 m/s

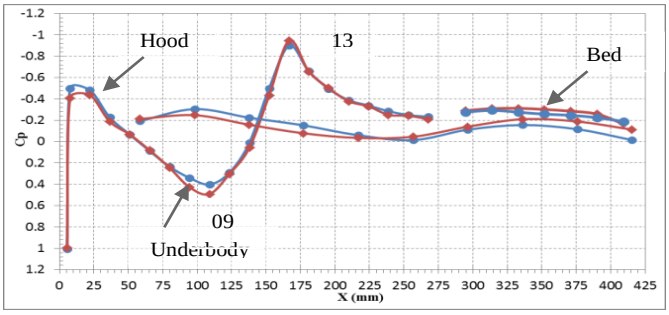

Figure 3.2 (a) Mean pressure coefficient distribution measured on the symmetry plane of the pickup At 25 m/s

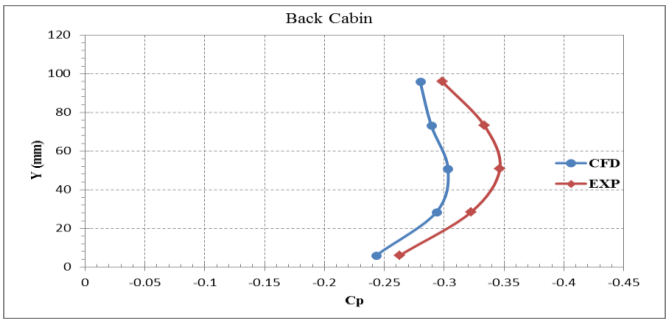

Figure 3.2 (b): Pressure distributions measured on the symmetry plane of the back surface of the cabin at 25 m/s

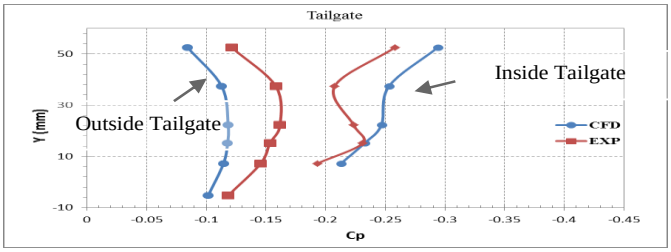

Figure 3.2 (c): Pressure coefficient distribution measured on the symmetry plane of the inside and outside surfaces of the tailgate of the pickup truck at 25 m/s

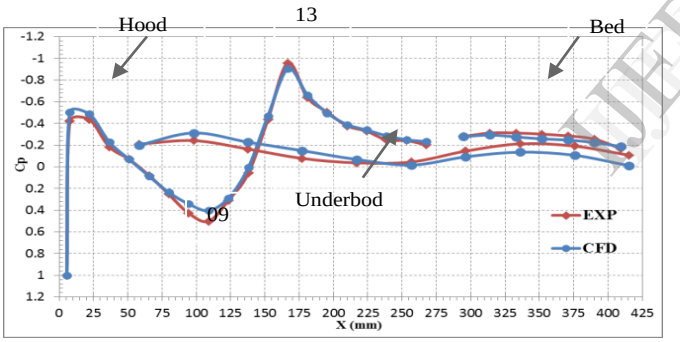

Figure 3.3 (a) Mean pressure coefficient distribution measured on the symmetry plane of the pickup At 30 m/s

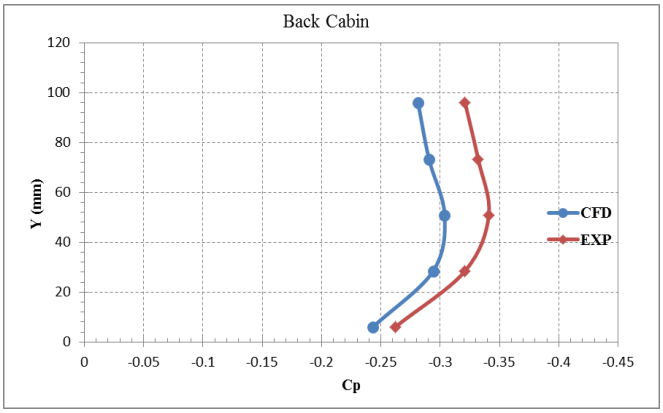

Figure 3.3 (b): Pressure distributions measured on the symmetry plane of the back surface of the cabin at 30 m/s

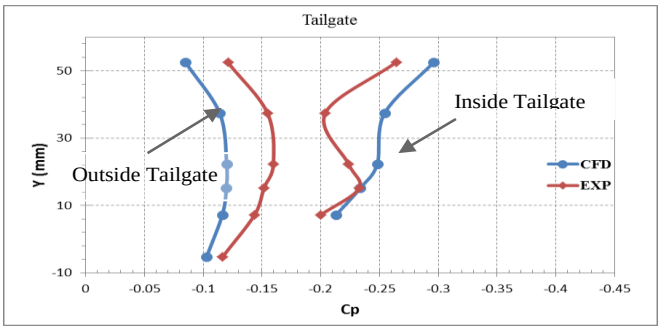

Figure 3.3 (c): Pressure coefficient distribution measured on the symmetry plane of the inside and outside surfaces of the tailgate of the pickup truck at 30 m/s

The mean pressure distribution on the engine hood and passenger cabin is marked "Cab." It shows the expected features. At the front bumper there is a stagnation point, $Cp = 1$. The flow accelerates to a local maximum velocity around the front of the engine compartment where the local pressure coefficient is ~ -0.4. On the hood the flow speed decreases and the pressure increases to a local maximum of the pressure coefficient, Cp = 0.5, at the lower corner of the windshield (point 9 in Figure 3.1(a), 3.2(a), 3.3(a)). On the windshield the flow speed increases and the pressure coefficient decrease to a minimum value of -0.9 at the top of the windshield (point 13 in Figure 3.1(a), 3.2(a), 3.3(a)).

On the top of the cabin, the flow speed decreases and the pressure coefficient increases to -0.2. The pressure distribution on the bottom of the pickup truck is marked "Underbody" in Figure 3.1(a), 3.2(a), 3.3(a). The pressure coefficient varies slightly with local minima (Cp ~ -0.2) at x ~ 100 *mm* and x ~ 350 *mm*, which correspond to the locations of the wheels. The local decrease of the pressure on the bottom surface at the location of the wheels is attributed to the local acceleration of the underbody flow due to the reduced flow cross section area at the wheels. The pressure coefficient in the pickup truck bed is marked "Bed" in Figure 3.1(a), 3.2(a), 3.3(a). The pressure coefficient is approximately -0.3 and increases to ~-0.2 towards the tailgate. The pressure coefficient in the bed shows a weak but significant Reynolds number dependence. At the lowest Reynolds number tested the

pressure coefficient is lower by ~0.05 compared to the results at higher Reynolds numbers.

The pressure coefficients measured on the back surface of the cab are shown in Figure 3.1(b), 3.2(b), 3.3(b). At high Reynolds number the pressure coefficient has a minimum value (Cp ~ -0.35) at approximately the center of the base (z ~ 50 *mm*). The pressure coefficient increases towards the top of the cab and towards the bed surface. There is a significant decrease of the pressure coefficient (~- 0.05) at the lowest Reynolds number in the lower two thirds of the cab base (0 < z < 70 *mm*). This trend is reversed near the top of the cab base were the pressure coefficient increases to -0.14 at the lowest Reynolds number compared to Cp values of -0.30 and -0.32 at the intermediate and high Reynolds numbers, respectively.

The pressure coefficient distribution on the symmetry plane of the tailgate is shown in Figure 3.1(c), 3.2(c), 3.3(c). The results on the outside and inside surfaces of the tailgate are shown in the figure as marked. The pressure coefficient outside the bed shows good collapse of the data at the three Reynolds numbers tested. The minimum pressure coefficient of -0.17 is found at z ~ 25 *mm* and increases slightly to –0.12 at the top and the bottom edges of the tailgate. In contrast the pressure coefficient distribution on the inside surface of the tailgate shows slightly lower values (~ -0.025) at the lower Reynolds number.

In addition there is rapid decrease of the pressure coefficient at the edge of the tailgate, indicating a rapid acceleration of the flow in this region. Finally note that the mean pressure on the inside surface of the tailgate is lower than on the outside surface suggesting that the force acting on the tailgate is in the forward direction, reducing aerodynamic drag.

Velocity Measurements

Bed Flow

Figure 3.4(a) & Figure 3.4 (b) shows the mean velocity profiles in the symmetry plane of the flow over the bed for the three Reynolds number considered in this investigation. The plots shows the results of two separate tests one for the flow outside the bed and the other for the flow inside the bed. The data at different Reynolds numbers collapse on a single curve indicating that Reynolds number effects are very small at the present flow conditions.

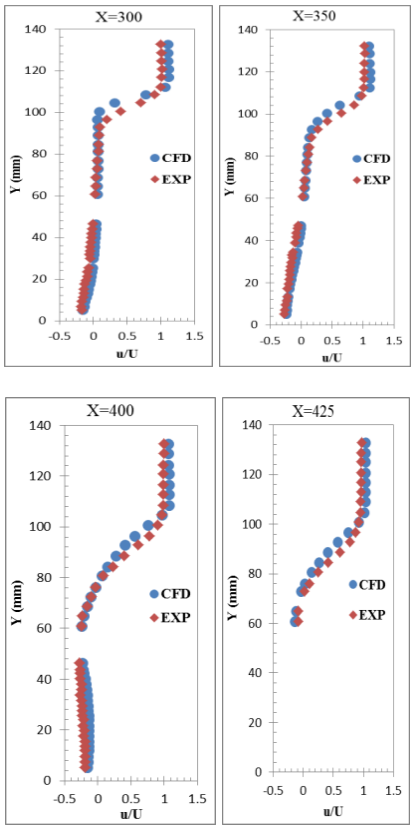

Figure 3.4 (a) Mean velocity profiles of the flow in the symmetry plane of the wake over the bed: streamwise velocity at 30 m/s

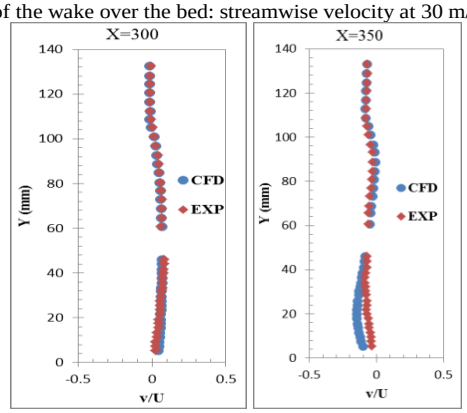

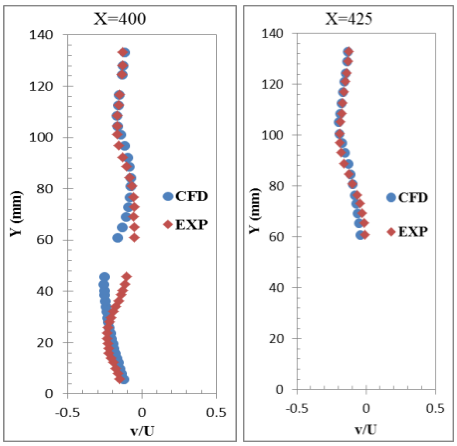

Figure 3.4 (b) Mean velocity profiles of the flow in the symmetry plane of the wake over the bed: vertical velocity at 30 m/s

Figure 3.4 (a) & Figure 3.4 (b) shows the streamwise velocity profiles at several downstream locations. Note that the cab base is located at x = 280 *mm*. Inside the bed the *u* velocities are negative indicating an upstream flow. It is clear from the *u/U* and *v/U* profiles that the flow enters the bed near the tailgate and leaves it near the cab base. The maximum reversed velocity inside the bed is approximately 0.32 times the free stream speed.

Tailgate Flow

The mean velocity profiles for the flow behind the tailgate at the symmetry plane are shown in Figure 3.5 (a) & 3.5 (b). The downstream evolution of *u/U* shown in Figure 3.5 (a) indicates a reduction of the maximum velocity in the underbody flow as the shear layer width increases. Moreover, the maximum upstream velocity in the wake of the tailgate is very small (i.e. *u/U* = -0.05) compared to the flow behind the cab (i.e. *u/U* = -0.3). The *v/U* velocity profiles are shown in Figure 3.5 (b). These results show a downward flow in the symmetry plane. The downstream location of the negative maxima, *v/U* = 0.35, is approximately at x ~ 500 *mm*, which corresponds to 68 *mm* from the tailgate.

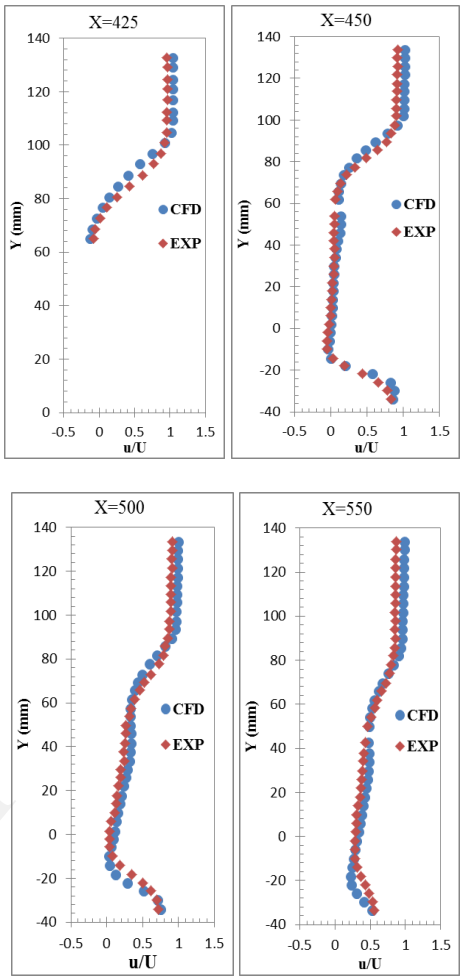

Figure 3.5 (a) Mean velocity profiles in the symmetry plane of the wake behind the tailgate: streamwise velocity at 30 m/s

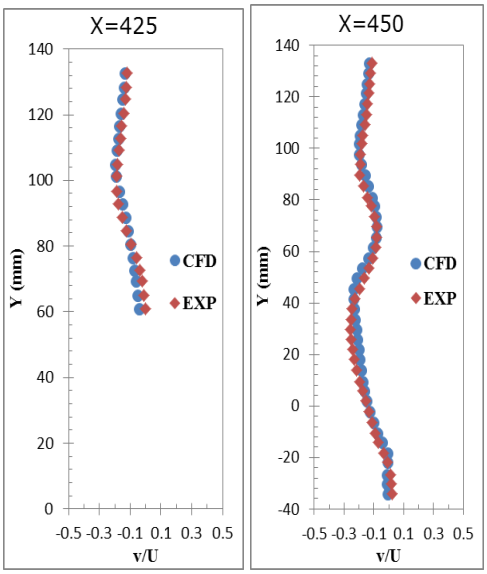

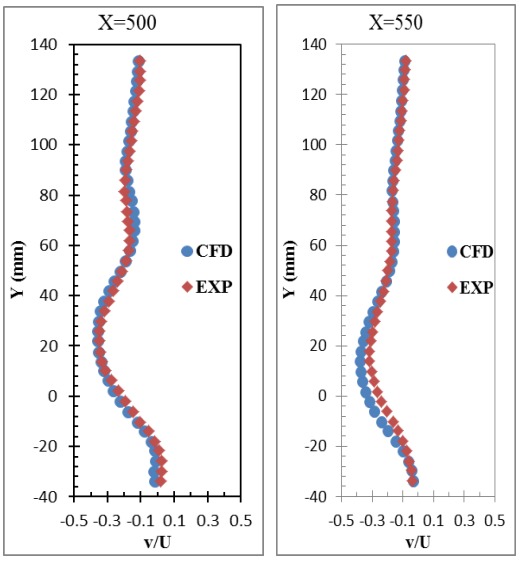

Figure 3.5 (b) Mean velocity profiles in the symmetry plane of the wake behind the tailgate: vertical velocity at 30 m/s

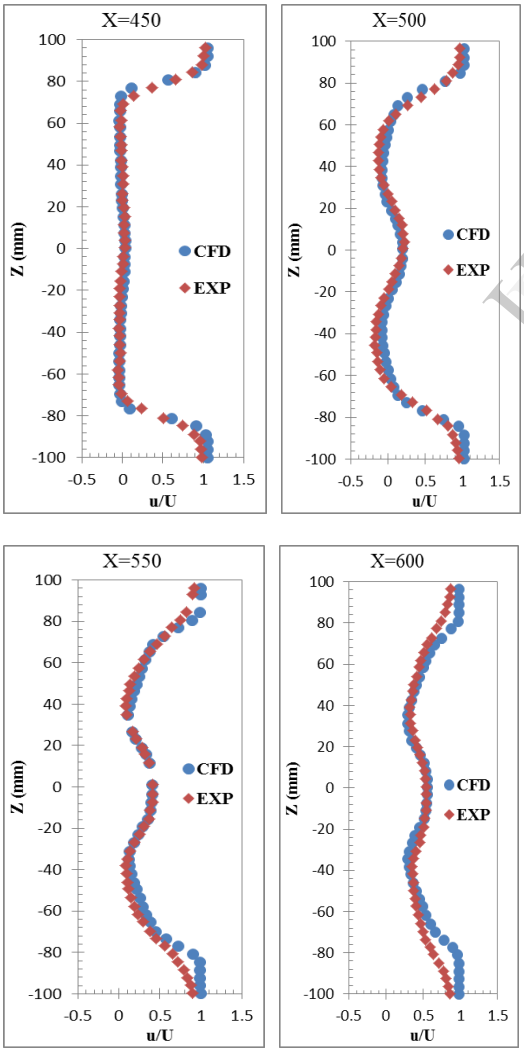

Figure 3.6 (a) Mean velocity profiles of the flow in the z = 15 *mm* plane of the wake behind the tailgate: streamwise velocity component at 30 m/s

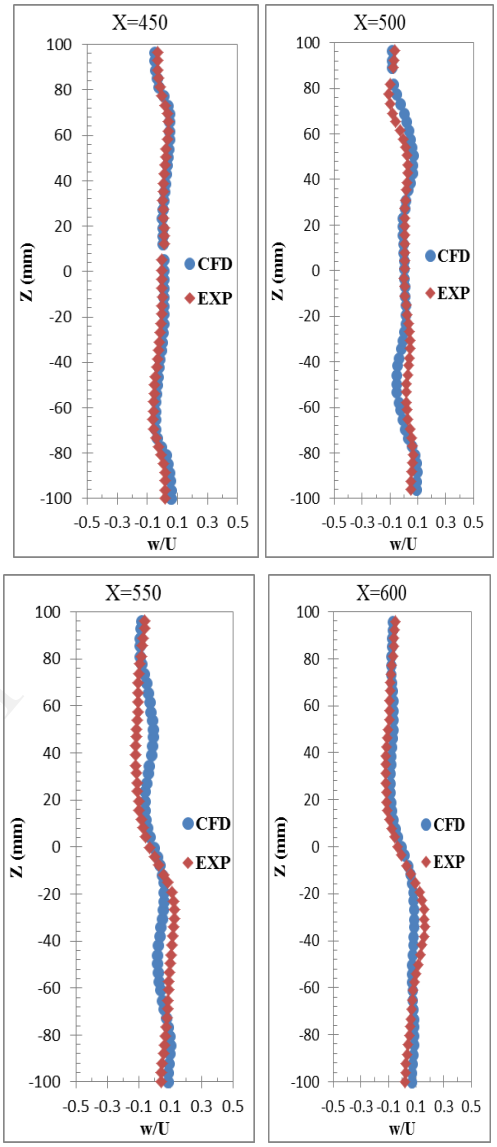

Figure 3.6 (b) Mean velocity profiles of the flow in the z = 15 *mm* plane of the wake behind the tailgate: lateral velocity component at 30 m/s

Mean velocity profiles in horizontal plane z = 15 *mm* behind the tailgate are shown in Figure 3.6 (a) & 3.6 (b). The downstream evolution of *u/U* in Figure 3.6 (a) shows the evolution of shear layers at the side edges of the tailgate and a region of high velocity at the symmetry plane. The velocity in the symmetry plane increases very rapidly with downstream distance reaching a value of 0.74 at x = 700 *mm* (not shown in the plot). Reversed flow regions are found at x = 500 *mm* on both sides of the

symmetry plane. Profiles of the normalized mean lateral velocity, *w/U*, are shown in Figure 3.6 (b).

The magnitude increases with downstream distance reaching a maximum value of approximately ±0.15 at x = 600 *mm* and decreasing farther downstream.

The results shown for pressure measurements and velocity measurements are closely matching the experimental results [1] [5] and hence we can conclude that CFD can be adopted as the alternative for the experimentations which are most expensive in all the ways.

Coefficient of Lift & Coefficient of Drag

The coefficient of lift and drag and coefficient of lift are recorded as follows for 18 m/s, 25 m/s, 30 m/s**.**

Table 3.1 C_D and C_F

	C_D	C_L
18 m/s	0.30	0.29
25 m/s	0.30	0.20
30 m/s	0.30	0.29

4. CONCLUSIONS

An investigation of the flow in the near wake of a pickup truck model has been conducted. The main conclusions of the investigation are:

- Mean pressure data show the expected behavior at the front of cab, and a cab base pressure coefficient in the range Cp ~ -0.25 to -0.35.
- The mean pressure distribution on the tailgate show a lower pressure coefficient on the inside surface compared to the outside surface suggesting that the tailgate reduces aerodynamic drag.
- The pressure fluctuations at the cab base are very low and increases significantly towards the back of the bed and the tailgate top edge.
- Mean velocity field measurements in the symmetry plane show a recirculating flow region over the bed bounded by the cab shear layer. The cab shear layer does not interact directly with the tailgate..
- The underbody flow results in the formation of a strong shear layer in the near wake.
- One of the more striking features of the pickup truck flow is the downwash on the symmetry plane behind the tailgate, and the formation of two smaller recirculating flow regions on both sides of the symmetry plane. These features are consistent with the formation of streamwise vortices in the wake.
- An approach of this nature would greatly reduce design time and make CFD a more feasible option.

5. REFERENCES

[1]. Bahram Khalighi, Abdullah .M. Al-Garni, and Luis P. Bernal, "Experimental Investigation of the Near Wake of a Pick-up Truck", Society of Automotive Engineers, journal number 2003-01-0651.

[2]. GridZ™ Version 4.5 Manual, Zeus Numerix Pvt Ltd, March 2009

[3]. FlowZ- Pressure Based™ Version 1.4 Manual, Zeus Numerix Pvt Ltd, March 2009

[4]. ParaView User's manual for v3.14.1 64-bit, Sandia National Laboratories

[5]. Bahram Khalighi, General Motors R&D Center, VAD Lab, "Pickup Truck Aerodynamics A PIV Study"

[6]. Anderson, J. D. (1995). *Computational Fluid Dynamics: The Basics with Applications*, McGraw-Hill, New York

[7]. Suhas.V.Patankar (1980). Numerical heat Transfer and Fluid Flow: Hemisphere Publishing Corporation, New York

[8]. T. J. Craft "Pressure-Velocity Coupling", School of Mechanical Aerospace and Civil Engineering, Advanced Modelling & Simulation: CFD